The N terminus and transmembrane segment S1 of Kv1.5 can coassemble with the rest of the channel independently of the S1–S2 linkage

Received for publication, May 18, 2018, and in revised form, August 14, 2018 Published, Papers in Press, August 17, 2018, DOI 10.1074/jbc.RA118.004065

Shawn M. Lamothe, Aja E. Hogan-Cann, Wentao Li, Jun Guo, Tonghua Yang, Jared N. Tschirhart, and Shetuan Zhang[1]

From the Department of Biomedical and Molecular Sciences, Queen's University, Kingston, Ontario K7L 3N6, Canada

Edited by Mike Shipston

The voltage-gated potassium channel Kv1.5 belongs to the Shaker superfamily. Kv1.5 is composed of four subunits, each comprising 613 amino acids, which make up the N terminus, six transmembrane segments (S1–S6), and the C terminus. We recently demonstrated that, in HEK cells, extracellularly applied proteinase K (PK) cleaves Kv1.5 channels at a single site in the S1–S2 linker. This cleavage separates Kv1.5 into an N-fragment (N terminus to S1) and a C-fragment (S2 to C terminus). Interestingly, the cleavage does not impair channel function. Here, we investigated the role of the N terminus and S1 in Kv1.5 expression and function by creating plasmids encoding various fragments, including those that mimic PK-cleaved products. Our results disclosed that although expression of the pore-containing fragment (Frag(304–613)) alone could not produce current, coexpression with Frag(1–303) generated a functional channel. Immunofluorescence and biotinylation analyses uncovered that Frag(1–303) was required for Frag(304–613) to traffic to the plasma membrane. Biochemical analysis revealed that the two fragments interacted throughout channel trafficking and maturation. In Frag(1–303)+(304–613)-coassembled channels, which lack a covalent linkage between S1 and S2, amino acid residues 1–209 were important for association with Frag(304–613), and residues 210–303 were necessary for mediating trafficking of coassembled channels to the plasma membrane. We conclude that the N terminus and S1 of Kv1.5 can attract and coassemble with the rest of the channel (*i.e.* Frag(304–613)) to form a functional channel independently of the S1–S2 linkage.

Voltage-gated potassium (Kv)[2] channels play important roles in all excitable cells. Kv1.5 channels are a member of the Shaker superfamily of Kv channels. They are expressed in various tissues (1). In the heart, Kv1.5 is mainly expressed in the atria and conducts the ultra-rapidly activating delayed rectifier K^+ current (I_{Kur}), which is important for atrial repolarization (2, 3). In pulmonary artery smooth muscle cells, Kv1.5 plays an important role in regulating membrane potential and vascular tone (4, 5). Elucidating the biochemical and biophysical properties of Kv channels is important and represents an active area of research. In particular, it is fundamental to understand how each part of ion channel structure contributes to assembly, trafficking, function, and regulation.

A single Kv channel is composed of four α-subunits, often identical, that assemble to form a tetramer (6, 7). Each α-subunit contains six transmembrane segments, S1–S6, with N and C termini located intracellularly. Each structural component contributes distinctively to channel function. For example, the S4 segment acts as the voltage sensor (8). The linker of S5 and S6 contributes to forming the K^+-selective permeation pore (9). However, the roles of other structural components such as the N terminus and S1 segment in expression and function are less well understood.

We recently demonstrated that Kv1.5 channels can be cleaved at a single site in the S1–S2 linker by extracellularly applied proteinase K (PK) into an N-fragment that contains the N terminus and S1 and a C-fragment that contains S2 to the C terminus. However, PK-cleaved Kv1.5 still generates robust current (10). In the current study, we created plasmids encoding Frag(1–303) (fragment containing amino acid residues 1–303, which make up the N terminus and S1 segment) and the pore-containing Frag(304–613) (fragment containing amino acid residues 304–613, which make up S2–S6 and the C terminus) as well as further defined smaller fragments to investigate the role of the N terminus and S1 in Kv1.5 trafficking and function. Our results showed for the first time that even when the linkage within the S1–S2 linker was absent, Frag(1–303) was able to attract and assemble with Frag(304–613) to form a functional channel. Specifically, residues 1–209 of Frag(1–303) interacted with the independent Frag(304–613). Residues 210–303 (the remaining N terminus and S1 of Frag(1–303)) mediated channel trafficking to the plasma membrane. Further analysis indicated that residues 210–240 of the N terminus were required for the expression of S1–S2 linker-intact Kv1.5 channels in the plasma membrane. These results revealed novel

This work was supported by Natural Sciences and Engineering Research Council of Canada Grant RGPIN-2018-05037 (to S. Z.). The authors declare that they have no conflicts of interest with the contents of this article.

[1] To whom correspondence should be addressed: Dept. of Biomedical and Molecular Sciences, Queen's University, 18 Stuart St., Kingston, Ontario K7L 3N6, Canada. Tel.: 613-533-3348; Fax: 613-533-6880; E-mail: shetuan.zhang@queensu.ca.

[2] The abbreviations used are: Kv, voltage-gated potassium; BFA, brefeldin A; co-IP, coimmunoprecipitation; HEK, human embryonic kidney; PK, proteinase K; Tuni, tunicamycin; Frag, fragment; $I_{Kv1.5}$, Kv1.5 current; Kv1.5-HEK, Kv1.5-expressing HEK; *g-V*, activation-voltage; hERG, human ether-a-go-go–related gene; pF, picofarad; MEM, minimum essential medium; PMSF, phenylmethylsulfonyl fluoride; HRP, horseradish peroxidase; GAPDH, glyceraldehyde-3-phosphate dehydrogenase.

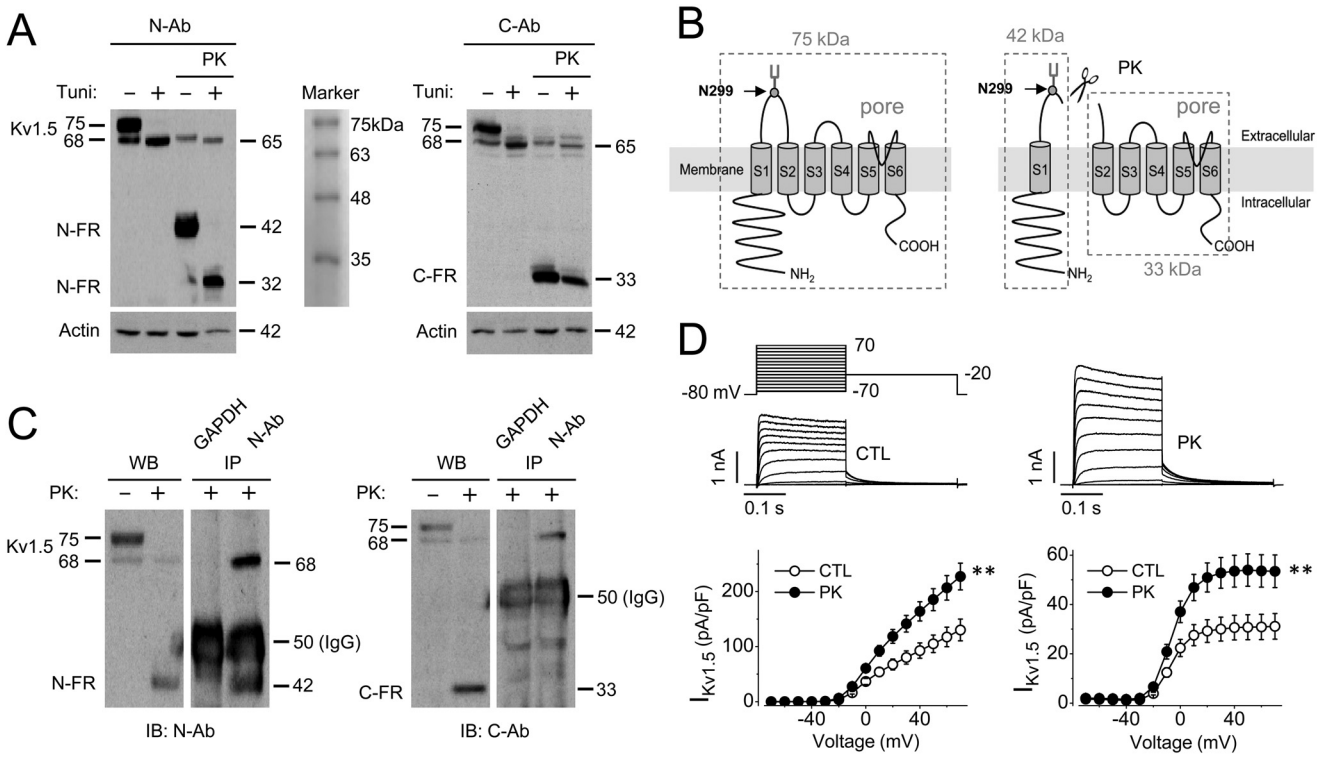

Figure 1. PK cleaves Kv1.5 at the S1–S2 linker and increases $I_{Kv1.5}$. *A*, Western blots depicting Kv1.5 expression following PK treatment (200 μg/ml, 20 min, 37 °C) of Kv1.5-HEK cells cultured with or without Tuni (10 μg/ml) for 48 h ($n = 6$). Proteins were detected using anti-N-terminal (*N-Ab*) or anti-C-terminal (*C-Ab*) Kv1.5 antibody. Actin was used as a loading control. Molecular mass marker (*Marker*) is shown in the *middle*. *B*, schematic illustration of Kv1.5 PK cleavage. *C*, co-IP assay showing that the N- (*N-FR*) and C-fragments (*C-FR*) do not associate after PK cleavage. Whole-cell proteins were extracted from PK-treated WT Kv1.5-HEK cells, and an anti-N-terminal Kv1.5 antibody was added to precipitate the N-fragment and associated proteins. Although the N-fragment was detected in the precipitate, the C-fragment was not detected. Western blotting (*WB*) of uncleaved and PK-cleaved Kv1.5 is shown to indicate the fragments. GAPDH was used as the control. *IP*, immunoprecipitation; *IB*, immunoblotting. The same results were obtained from five co-IP experiments. *D*, $I_{Kv1.5}$ in control (*CTL*) and PK-treated cells. The voltage protocol is shown above the current traces, and the summarized current-voltage (*I-V*) and *g-V* relationships are shown beneath the current traces ($n = 36$ in control; $n = 35$ in PK cleavage; **, $p < 0.01$ at 0 mV and above). *Error bars* represent S.E.

roles of the N terminus and S1 in Kv1.5 channel trafficking and assembly.

Results

The Kv1.5 channel is cleaved in the S1–S2 linker by PK

Using Western blot analysis and whole-cell patch clamp method, we examined the effects of PK treatment on the expression and function of Kv1.5 channels. Kv1.5 channel proteins exist in two forms: the mature form, which is localized in the plasma membrane, and the immature form, which is localized intracellularly. It is the membrane-localized, mature protein that conducts Kv1.5 current ($I_{Kv1.5}$) (10, 11). Kv1.5 is synthesized as a 65-kDa protein. It undergoes core glycosylation to become a 68-kDa immature channel and further complex glycosylation to become a 75-kDa mature channel localized in the plasma membrane (Fig. 1*A*, *lane 1*). *N*-Glycosylation of Kv1.5 occurs at Asn-299 (GenBank accession number NM_002234.3) within the S1–S2 linker (10). Glycosylation is not a prerequisite for the trafficking of Kv1.5 channels to the plasma membrane (10). Thus, after inhibition of glycosylation with tunicamycin (Tuni; 10 μg/ml, 48 h), both mature (plasma membrane) and immature (intracellular) channels display as a 65-kDa band (Fig. 1*A*, *lane 2*). PK, which cannot permeate the cell membrane, cleaves cell-surface protein when applied extracellularly (12). For normally glycosylated Kv1.5 channels, treatment of intact Kv1.5-expressing human embryonic kidney (HEK) (Kv1.5-HEK) cells with PK (200 μg/ml, 20 min, 37 °C) selectively abolished the 75-kDa Kv1.5 band without affecting the 68-kDa Kv1.5 band (Fig. 1*A*, *lane 3*). The disappearance of the 75-kDa band was accompanied by the appearance of a 42-kDa N-fragment (detected using an N terminus–targeting Kv1.5 antibody; Fig. 1*A*, *left*, *lane 3*) and a 33-kDa C-fragment (detected using a C terminus–targeting Kv1.5 antibody; Fig. 1*A*, *right*, *lane 3*). Resistance of the 68-kDa Kv1.5 protein to PK cleavage confirmed its intracellular location (Fig. 1*A*, *lane 3*). For unglycosylated channels (65-kDa; Tuni treatment), PK treatment cleaved the mature, plasma membrane–localized 65-kDa protein but not the immature, intracellularly localized 65-kDa protein (Fig. 1*A*, *lane 4*). As a result, PK treatment only decreased the intensity of the 65-kDa protein but did not abolish it. Cleavage of the unglycosylated plasma membrane Kv1.5 protein resulted in the appearance of a 32-kDa N-fragment (Fig. 1*A*, *left*, *lane 4*) and a 33-kDa C-fragment (Fig. 1*A*, *right*, *lane 4*). Thus, removal of glycosylation reduced the N-fragment from 42 to 32 kDa but did not affect the size of the C-fragment (Fig. 1*A*). These results indicate that the glycosylation site (Asn-299) is located within the N-fragment. Together with ExPASy ProtParam analysis based on the fragment sizes, these data indicated that PK likely cleaves Kv1.5 at a site between Asn-299 and the carboxyl end of the S1–S2 linker (Fig. 1*B*).

To determine whether the PK-generated N- and C-fragments associate with each other, we performed a coimmuno-

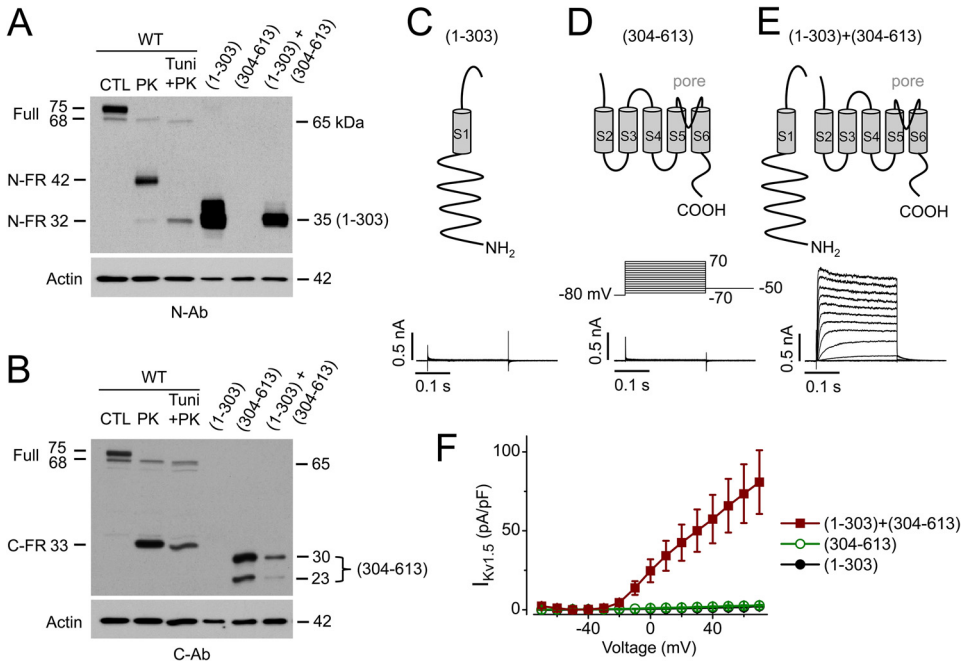

Figure 2. Expression and function of Kv1.5 N- (*N-FR*) and C-fragments (*C-FR*). *A* and *B*, Western blots of Frag(1–303) and Frag(304–613) along with full-length Kv1.5 protein without and with PK cleavage from cells treated without or with Tuni treatment (10 μg/ml, 48 h). Kv1.5 proteins were detected with an N-terminal (*N-Ab*) or C-terminal antibody (*C-Ab*). Actin was used as a loading control ($n = 8$). *C–E*, schematics illustrating Frag(1–303) and Frag(304–613) as well as corresponding current traces upon independent expression or coexpression. The voltage protocol is shown in the *inset* above the current traces. *F*, summarized current-voltage relationships of currents generated by Frag(1–303) ($n = 8$), Frag(304–613) ($n = 10$), and Frag(1–303)+(304–613) ($n = 14$). *Error bars* represent S.E. *CTL*, control.

precipitation (co-IP) assay. Our results indicated that the PK-generated N-fragment (42 kDa) and C-fragment (33 kDa) of Kv1.5 did not associate (Fig. 1*C*) (10). Interestingly, PK cleavage of Kv1.5 did not impair channel function but instead led to an increase in $I_{Kv1.5}$ without affecting the activation-voltage (*g-V*) relationships (Fig. 1*D*). The *g-V* relationships were fit to the Boltzmann function. The half-maximal activation voltage and the slope factor were -6.95 ± 0.91 mV and 5.55 ± 0.34 in control ($n = 36$) and -5.82 ± 0.99 mV and 6.12 ± 0.30 in the PK cleavage group ($n = 35$, $p > 0.05$).

Coexpression of fragments that mimic PK-generated products produces a functional channel

For PK-cleaved full-length Kv1.5 channels, it was of interest to determine whether the C-fragment of Kv1.5, which contains the pore region of the channel, was solely responsible for channel function or whether the N- and C-fragments function together. To this end, we created two independent plasmids in pcDNA3 vectors encoding Frag(1–303) and Frag(304–613) of Kv1.5 that mimic the PK cleavage products. Specifically, similar to PK-generated fragments, Frag(1–303) contains the N terminus (positions 1–247), S1 (positions 248–269), and part of the S1–S2 linker (positions 270–303; UniProt accession number P22460), which contains the glycosylation site (Asn-299) (Fig. 2). Frag(304–613) constitutes part of the S1–S2 linker, the S2–S6 transmembrane segments, and the C terminus. Upon Western blot analysis, Frag(1–303) displayed a band of ~35 kDa (Fig. 2*A*), which is not affected by the removal of glycosylation by Tuni treatment (data not shown). Thus, Frag(1–303) is not glycosylated for unknown reasons. Frag(304–613) displays 30- and 23-kDa bands (Fig. 2*B*). The 30-kDa band is the full-length C-fragment, and the 23-kDa band is a degradation product that can be abolished by inhibiting protein degradation with lactacystin (10 μM) (data not shown). Thus, Frag(304–613) displayed a molecular mass (30 kDa) similar to the PK-generated C-fragment (33 kDa) (Fig. 2*B*). However, Frag(1–303) displayed a molecular mass (35 kDa) similar to the PK-generated N-fragment of Tuni-treated Kv1.5-HEK cells (32 kDa) due to a lack of glycosylation (Fig. 2*A*).

We measured the current produced by expressing Frag(1–303) and Frag(304–613) independently or together in HEK 293 cells. As expected, no current was measurable when Frag(1–303) was expressed independently as it lacks the pore region of the channel (Fig. 2*C*). However, independent expression of Frag(304–613) also did not produce current despite containing the pore region (Fig. 2*D*). Interestingly, when Frag(1–303) and Frag(304–613) were coexpressed, robust current was detected (Fig. 2, *E* and *F*).

Frag(304–613) requires Frag(1–303) to traffic to the membrane and form functional channels

Western blot analysis of whole-cell proteins extracted from Frag(1–303)- and/or Frag(304–613)-expressing cells showed that the two fragments are robustly expressed regardless of whether they are independently expressed or coexpressed (Fig. 3*A*, *left*). However, in cells coexpressed with both fragments, a full-length Kv1.5 protein (75 kDa glycosylated or 65 kDa unglycosylated) was not observed (Fig. 3*A*, *left*), indicating that the current is generated by a Frag(1–303)+(304–613)-coassembled channel. Frag(304–613) contains the pore region but did not generate current when expressed alone. To determine whether Frag(304–613) requires Frag(1–303) for trafficking to

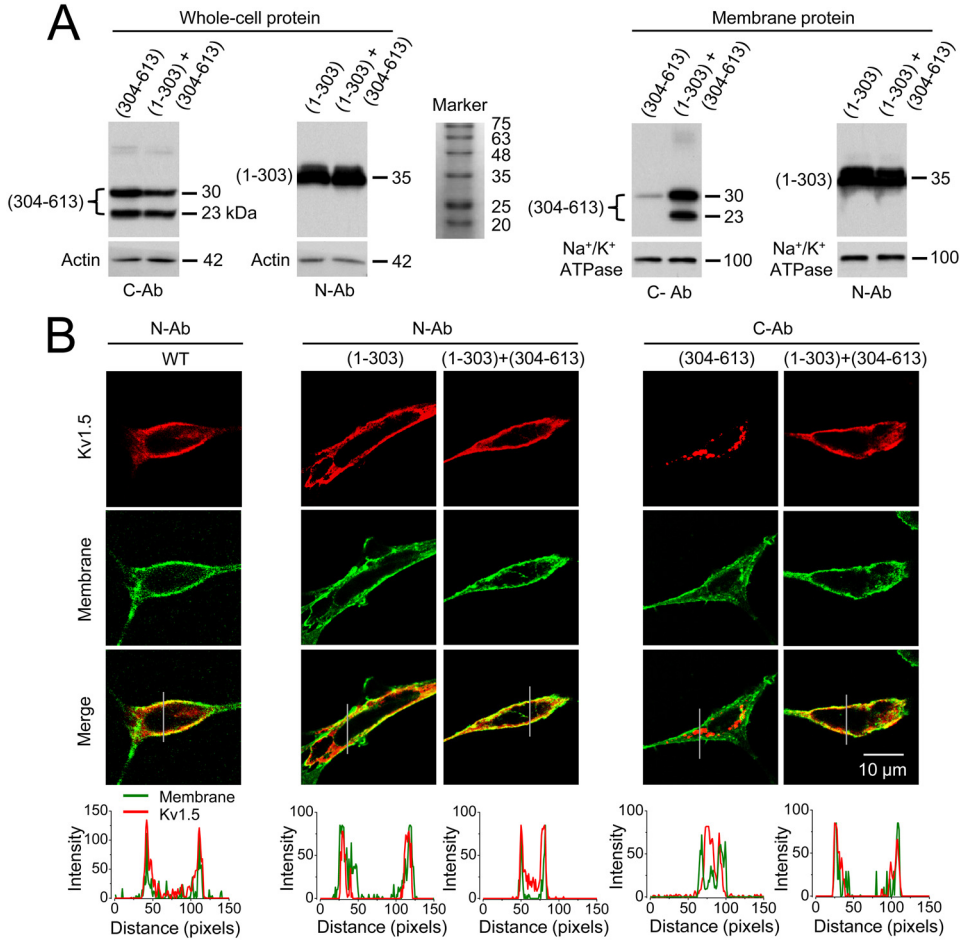

Figure 3. Frag(304–613) requires Frag(1–303) to traffic to the plasma membrane. *A*, Western blots depicting total expression (*left*) and membrane expression (*right*) of Frag(1–303) and Frag(304–613) expressed independently or together ($n = 6$). Actin and Na^+/K^+-ATPase were used as loading controls for total and membrane proteins, respectively. Molecular mass marker (*Marker*) is shown in the *middle*. *B*, confocal images portraying the localization of WT Kv1.5, Frag(1–303), or Frag(304–613) relative to the plasma membrane ($n = 4$). WT Kv1.5 was detected with the N-terminal antibody and is depicted in *red*. Frag(1–303) and Frag(304–613), detected with N-terminal (*N-Ab*) and C-terminal (*C-Ab*) antibodies, respectively, are depicted in *red*. Cell membranes are shown in *green*. Fluorescence intensities of WT Kv1.5, Frag(1–303), and/or Frag(304–613) and the membrane in the *line* across the cells were quantified by ImageJ and are shown beneath the representative images.

the plasma membrane, we isolated membrane protein using a biotinylation method. Frag(304–613) was barely detected in the membrane protein when it was independently expressed (Fig. 3*A*, *right*). In contrast, when both fragments were coexpressed, Frag(304–613) was robustly detected in the isolated membrane protein (Fig. 3*A*, *right*). In contrast, Frag(1–303) was detected in the membrane protein regardless of whether it was independently expressed or coexpressed with Frag(304–613) (Fig. 3*A*, *right*). These results indicate that Frag(1–303) mediates the trafficking of Frag(304–613) to the plasma membrane. This notion was confirmed by data from immunofluorescence microscopy experiments. As shown in Fig. 3*B*, Frag(1–303) was able to traffic to the plasma membrane when expressed alone or coexpressed with Frag(304–613). However, Frag(304–613) was retained intracellularly when expressed alone but was present on the plasma membrane when it was coexpressed with Frag(1–303) (Fig. 3*B*).

Frag(1–303) and Frag(304–613) of Kv1.5 channels interact during channel trafficking and maturation

To determine the association between Frag(1–303) and Frag(304–613) of Kv1.5, we performed co-IP assays of whole-cell proteins extracted from cells coexpressing both fragments. Unlike the PK-produced fragments (Fig. 1*C*), Frag(1–303) and Frag(304–613) associated with one another (Fig. 4*A*). In a separate set of experiments, Frag(1–303)- and Frag(304–613)-coexpressing cells were treated with PK (200 μg/ml, 20 min, 37 °C) prior to protein extraction and co-IP assays. The association between Frag(1–303) and Frag(304–613) was still present in the PK-treated cells (Fig. 4*B*), suggesting that, unlike wildtype (WT) Kv1.5 channels, the association between Frag(1–303) and Frag(304–613) is not in the S1–S2 linker. Additionally, after cotransfection of HEK cells with Frag(1–303) and Frag(304–613) plasmids, we treated transfected cells with brefeldin A (BFA; 10 μM) for 12 h to inhibit protein trafficking from the endoplasmic reticulum to the Golgi apparatus during maturation (13) and thus eliminated the cell-surface expression of both fragments. Co-IP analysis indicated that the two fragments are still associated in the presence of BFA (Fig. 4*C*). Therefore, Frag(1–303) and Frag(304–613) appear to associate intracellularly before they traffic through the Golgi apparatus to the plasma membrane. Additionally, consistent with the results shown in Figs. 2, *A* and *B*, and 3*A*, coexpression of Frag(1–303) and Frag(304–613) did not

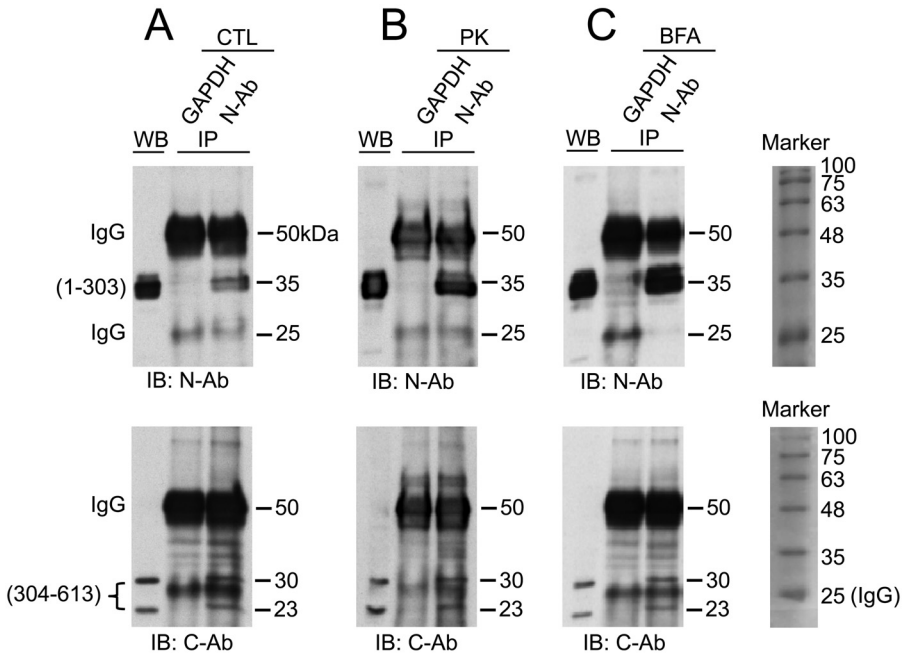

Figure 4. Frag(1–303) and Frag(304–613) associate intracellularly. Twenty-four hours after cotransfection of Frag(1–303) and Frag(304–613) into HEK cells with various treatments, an anti-N-terminal antibody (*N-Ab*) was used to immunoprecipitate (*IP*) Frag(1–303) and associated proteins from whole-cell lysates. Frag(1–303) and Frag(304–613) were detected in the precipitates upon immunoblotting (*IB*) with either anti-N-terminal or anti-C-terminal antibody (*C-Ab*) in untreated (*A*; *CTL*, control; $n = 3$), PK-treated (*B*; $n = 3$), or BFA-treated (*C*; $n = 3$) cells. GAPDH was used as a control for anti-N-terminal antibody. IgG was used as a loading control for co-IP assays. For clarity, IgG (25 kDa) in the *lower panels* is not labeled. Molecular mass markers (*Marker*) are shown on the *right*. In the *lower panels*, although IgG bands (50 and 25 kDa) are comparable, the 23- and 30-kDa bands coimmunoprecipitated with anti-N-terminal antibody but not GAPDH. *WB*, Western blotting.

generate a band close to the full-length channel (*e.g.* 75 or 65 kDa; Fig. 4), suggesting that, unlike WT, Frag(1–303) and Frag(304–613) do not interact in a covalent manner at the S1–S2 linker.

Residues 1–209 and 210–303 are important for interaction and trafficking, respectively, of coassembled channels

Our data so far indicate that Frag(1–303) interacts and coassembles with Frag(304–613), mediating trafficking of coassembled channels to the plasma membrane. To further understand the interaction between Frag(1–303) and Frag (304–613), we separated Frag(1–303) into two smaller fragments, Frag(1–209) and Frag(210–303). The separation site was selected based on previous works demonstrating that Kv1.5 with truncation of the N terminus up to residue 209 (ΔN209; contains residues 210–613) produces a functional channel with robust current (14, 15). This indicates that residues 1–209 are not essential for Kv1.5 trafficking and function provided that the rest of the channel (residues 210–613) is synthesized as a single entity. On Western blots, Frag(1–209) displayed a 30-kDa single protein band, whereas Frag(210–303) displayed two protein bands, a 19-kDa band and a 12-kDa band (Fig. 5*A*). In an attempt to produce functional channels, Frag(1–209), Frag(210–303), or both were cotransfected with Frag(304–613) in HEK cells. However, none of these combinations produced a current (Fig. 5*B*).

Frag(210–303) contains the glycosylation site and displayed two protein bands (19 and 12 kDa). Tuni treatment eliminated the 19-kDa band but retained the 12-kDa band, indicating that Frag(210–303) undergoes glycosylation (Fig. 5*C*). Furthermore, treatment of cells with BFA abolished the 19-kDa band but retained the 12-kDa band, indicating that Frag(210–303) trafficked through the Golgi apparatus (Fig. 5*C*). Immunofluorescence microscopy experiments demonstrated that Frag(210–303) was able to traffic to the plasma membrane. In contrast, Frag(1–209) was retained intracellularly (Fig. 5*D*).

To determine whether Frag(1–209) or Frag(210–303) was able to associate with Frag(304–613), co-IP assays were performed. Although Frag(1–209) associated with Frag(304–613) (Fig. 5*E*), Frag(210–303) did not (Fig. 5*F*). These results demonstrate that, when S1 and S2 are not covalently linked, Frag (1–209) is important for association with Frag(304–613), and Frag(210–303) is important for mediating trafficking of Frag(304–613) to the plasma membrane. However, neither Frag(1–209) nor Frag(210–303) alone were able to reconstitute a functional channel with Frag(304–613). Rather, both must be conjoined as a single fragment (Frag(1–303)) to interact with Frag(304–613) and form a functional channel.

To examine whether Frag(1–209), Frag(210–303), or Frag (1–303) is able to interact with full-length Kv1.5 channel subunits, we independently expressed them with WT Kv1.5 and determined whether they can produce a dominant-negative effect on WT Kv1.5 function (16, 17). To this end, 0.5 μg of pcDNA3 (control) or plasmids encoding Frag(1–209), Frag(210–303), or Frag(1–303) was transfected into Kv1.5-HEK cells. Neither Frag(1–209) nor Frag(210–303) affected $I_{Kv1.5}$ (Fig. 6). However, Frag(1–303) significantly reduced $I_{Kv1.5}$ (Fig. 6). Thus, neither Frag(1–209) nor Frag(210–303) alone

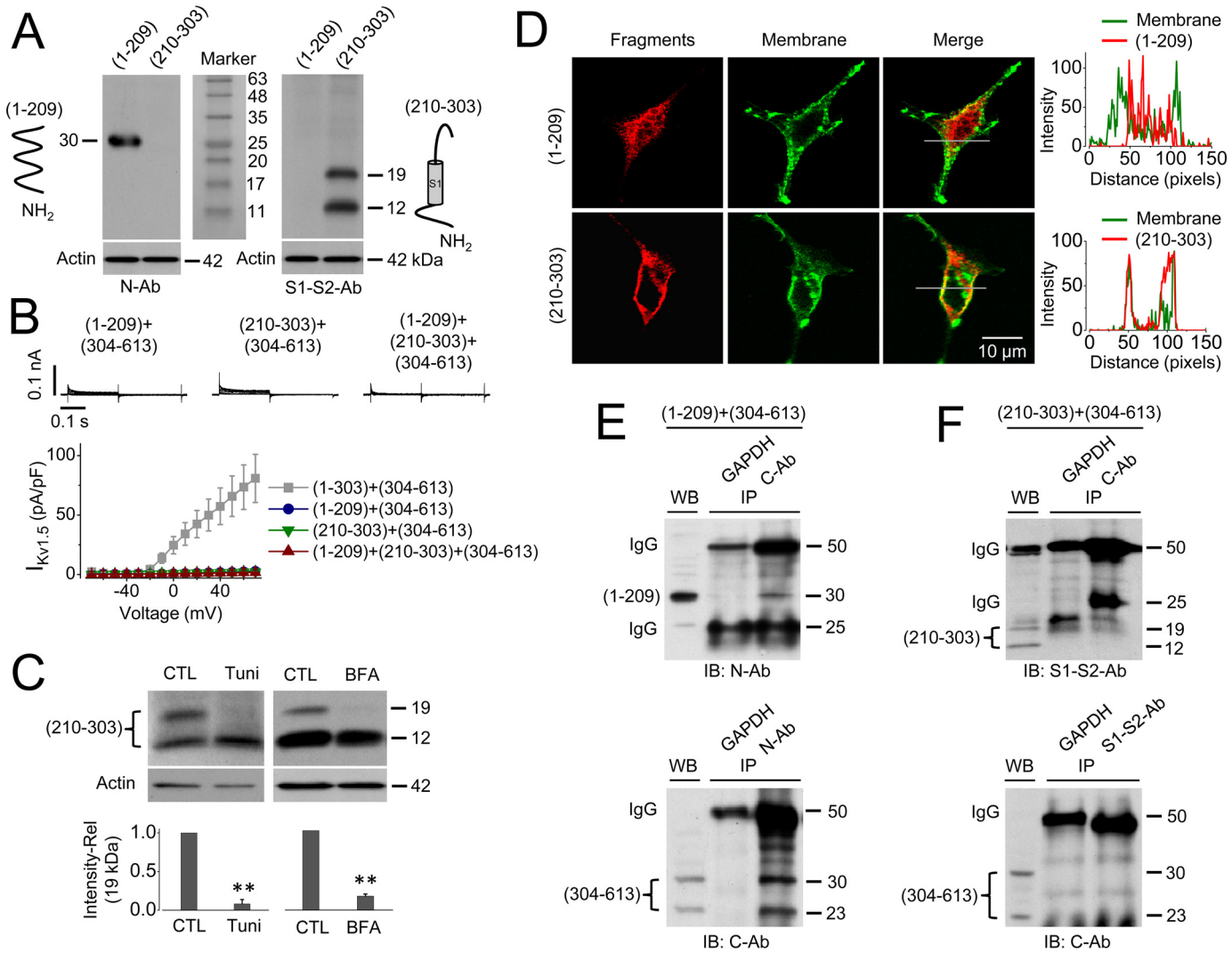

Figure 5. Amino acid residues 1–209 and 210–303 are important for interaction with and trafficking of Frag(304–613), respectively. *A*, Western blots of Frag(1–209) and Frag(210–303) expressed in HEK cells. Frag(1–209) was detected with an N-terminal antibody (*N-Ab*). Frag(210–303) was detected with an S1–S2 antibody (*S1-S2-Ab*). Schematic illustrations of Frag(1–209) and Frag(210–303) are depicted beside the Western blots. Actin was used a loading control ($n = 6$). Molecular mass marker (*Marker*) is shown in the *middle*. *B*, representative current traces from cells coexpressing Frag(1–209), Frag(210–303), or Frag(1–209)+(210–303) with Frag(304–613). Beneath the current traces are summarized *I-V* relationships of Frag(1–209)+(304–613) ($n = 5$), Frag(210–303)+(304–613) ($n = 6$), Frag(1–209)+(210–303)+(304–613) ($n = 6$), and Frag(1–303)+(304–613) (used as control; $n = 12$; same data as Fig. 2). *C*, Western blotting of Frag(210–303) from HEK cells cultured in standard condition (*CTL*), with Tuni (10 μg/ml) for 48 h ($n = 4$), or with BFA (10 μM) for 12 h ($n = 4$). Summarized bar graphs of the relative (*Rel*) densities of the upper band (19 kDa) are depicted below the representative Western blot images. *D*, confocal images demonstrating the localization of Frag(1–209) or Frag(210–303) relative to the plasma membrane ($n = 5$). Frag(1–209) was detected using the anti-N-terminal antibody, and Frag(210–303) was detected using the anti-S1–S2 antibody. Frag(1–209) and Frag(210–303) are depicted in *red*. The membrane is depicted in *green*. Fluorescence intensities of Frag(1–209) and Frag(210–303) and the membrane in the *line* across the cells were quantified by ImageJ and are shown on the *right*. *E*, co-IP assay demonstrating an interaction between Frag(1–209) and Frag(304–613). A C-terminal antibody (*C-Ab*) (*top*) or N-terminal antibody (*bottom*) was used to precipitate Frag(304–613) or Frag(1–209), respectively. An N-terminal antibody (*top*) or C-terminal antibody (*bottom*) was used to detect Frag(1–209) or Frag(304–613) in the precipitates, respectively ($n = 3$). *F*, co-IP assay to determine an interaction between Frag(210–303) and Frag(304–613). A C-terminal antibody (*top*) or S1–S2 antibody (*bottom*) was used to precipitate Frag(304–613) or Frag(210–303), respectively. An S1–S2 antibody (*top*) or C-terminal antibody (*bottom*) was used to detect Frag(210–303) or Frag(304–613) in the precipitates, respectively ($n = 3$). **, $p < 0.01$ *versus* standard condition. *Error bars* represent S.E. *WB*, Western blotting; *IB*, immunoblotting.

were able to interact and interfere with full-length Kv1.5 channels, but Frag(1–303) disrupted full-length Kv1.5 function.

The T1–S1 linker and/or S1 segment are important for plasma membrane expression of WT Kv1.5 channels

To further investigate the role of residues 1–303 in Kv1.5 trafficking and function, we utilized channel truncation strategies. We first truncated the N terminus up to residue 209 from full-length Kv1.5 to obtain ΔN209 mutant (Fig. 7*A*). This mutant contains residues 210–613, equivalent to the total residues of coexpressed Frag(210–303) and Frag(304–613) but with an intact S1–S2 linkage. Although coexpressed Frag(210–303) and Frag(304–613) (without S1–S2 linkage) did not produce functional channels (Fig. 5*B*), ΔN209 mutant (residues 210–613 with S1–S2 linkage) produced functional channels (Fig. 7*B*). This result indicates that when residues 210–303 are covalently linked with the rest of the channel they are sufficient to mediate Kv1.5 channel trafficking to form functional channels. Thus, residues 1–209 are not essential for membrane expression of Kv1.5 channels with the intact S1–S2 linker.

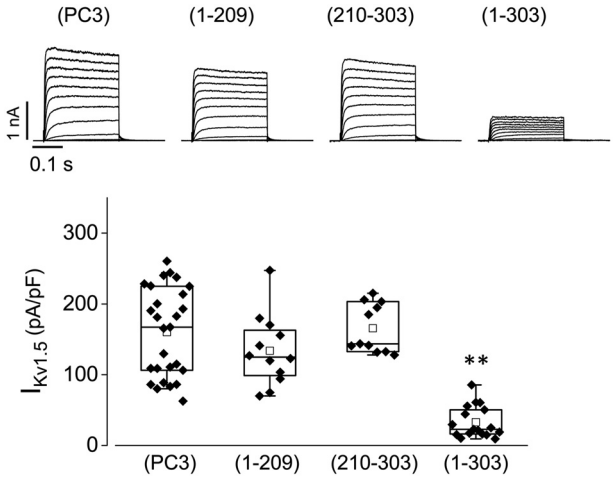

Figure 6. Dominant-negative suppression of WT Kv1.5 with Frag(1–303). Shown are the effects of transfecting empty pcDNA3 (*PC3*; control; $n = 27$) or plasmids encoding Frag(1–209) ($n = 12$), Frag(210–303) ($n = 11$), or Frag(1–303) ($n = 17$) into Kv1.5-HEK cells on $I_{Kv1.5}$. Representative current traces are depicted above the summarized box plots of current amplitudes upon 50-mV depolarization. **, $p < 0.01$ *versus* empty pcDNA3.

However, they are critical for the association of Frag(1–303) and Frag(304–613), which allows for trafficking of Frag(304–613) to the membrane (Fig. 5*E*). Residues 210–303 contain part of the N terminus (positions 210–247; known as the T1–S1 linker), S1 (positions 248–269), and part of the S1–S2 linker (positions 270–303; UniProt accession number P22460). To determine the role of the T1–S1 linker, we further shortened the N terminus to remove the T1–S1 linker but retain S1; we deleted the N terminus from amino acid 2 to 240 to construct the del(2–240) Kv1.5 mutant. The del(2–240) Kv1.5 mutant displayed two protein bands, a 45-kDa band and a 38-kDa band, in Western blots (Fig. 7*A*). Results from patch clamp experiments showed that del(2–240) Kv1.5 did not produce current (Fig. 7*B*). Treatment of HEK cells expressing the del(2–240) Kv1.5 mutant with either Tuni or BFA removed the 45-kDa band, indicating that the del(2–240) channel undergoes complex glycosylation and traffics through the Golgi apparatus (Fig. 7*C*). However, treatment of cells expressing del(2–240) Kv1.5 with PK (200 μg/ml, 20 min, 37 °C) did not affect the 45-kDa band, suggesting that the channel is not expressed in the plasma membrane (Fig. 7*C*). Results from immunofluorescence microscopy experiments indicated that, in contrast to ΔN209, which displayed plasma membrane expression, the del(2–240) Kv1.5 mutant was retained intracellularly (Fig. 7*D*). Thus, compared with ΔN209 (residues 210–613), further deletion of N-terminal residues 210–240 completely disrupted Kv1.5 membrane expression.

The biophysical properties of Frag(1–303)+(304–613)-coassembled Kv1.5 channels are different from WT channels

Our results showed that the N terminus interacts with other regions of Kv1.5 channels (Figs. 2–6), which is in line with previous studies demonstrating that the N terminus affects K^+ channel gating (18). Consistently, although WT Kv1.5 was inactivated to a similar extent (flat) upon 5-s depolarizing voltages between 0 and 90 mV, the N-terminal truncation Kv1.5 mutant ΔN209 displayed a U-shaped voltage dependence of inactivation (Fig. 8*A*), an observation that was also reported by Kurata *et al.* (14, 15). Interestingly, although Frag(1–303)+(304–613)-coassembled Kv1.5 channels contained the N terminus, they displayed a U-shaped voltage dependence of inactivation, similar to ΔN209 (Fig. 8*A*). The U-shaped voltage dependence of inactivation has been proposed to be a result of inactivation occurring from late closed states of the channel (19). Repeated depolarizations with short periods of negative voltage facilitate inactivation from late closed states, leading to excessive cumulative inactivation (14, 19). As shown in Fig. 8*B*, shuttling between 60 mV for 90 ms and −80 mV for 10-ms steps resulted in more cumulative inactivation in both ΔN209 and Frag(1–303)+(304–613)-coassembled channels than in WT Kv1.5 channels.

Discussion

Elucidating structure–function relationships is an essential step toward understanding the properties and regulation of Kv channels. Functional reconstitution from two nonoverlapping contiguous fragments represents a useful strategy to study the structure–function relationships for several transmembrane proteins such as β_2-adrenergic receptors, M1/M2 muscarinic acetylcholine receptors, lactose permease enzymes (20–23), and voltage-gated chloride channels (24–26). Upon functional reconstitution of transmembrane proteins from independent fragments, the contribution and behavior of different regions of the protein with regard to membrane insertion, protein interaction, assembly, trafficking, and function are further understood.

We previously demonstrated that, among various K^+ channels, PK selectively cleaves hERG at a site within the S5–pore linker into N- and C-fragments, leading to a complete loss of hERG function (27). In contrast, we found that PK also cleaves Kv1.5 at a site within the S1–S2 linker into N- and C-fragments but does not affect channel function (10). In this recently published work, we used a Kv1.5 stable cell line that displayed very large currents (~900 pA/pF upon 50-mV depolarization) to detect any loss of function. Due to the large currents, some cells displayed currents that exceeded the scale of the patch clamp amplifier (Axopatch 200B). As a result, the PK cleavage–induced increase in Kv1.5 current was overlooked in the previous study (10). To focus on the effects of PK cleavage on the functionality of Kv1.5 channels, we created a new stable Kv1.5-HEK cell line that expresses whole-cell current of 150–300 pA/pF upon 50-mV depolarization. Our data showed that Kv1.5 current increased upon PK cleavage (Fig. 1*D*). The mechanisms of PK cleavage–induced current increase are currently under investigation but are not due to the altered channel gating. PK cleavage did not affect the voltage dependence of activation (Fig. 1*D*). PK cleavage neither resulted in U-shaped voltage dependence of inactivation nor diminished Kv1.5 inactivation (data not shown). The present study focused on how Frag(1–303) and Frag(304–613) work together to form a functional channel. The mechanism underlying the formation of a functional channel after coexpression of the two DNA fragments remains to be fully elucidated. Our results showed that the two fragments are successfully coimmunoprecipitated (Fig. 4) unlike the fragments produced by PK treatment of full-

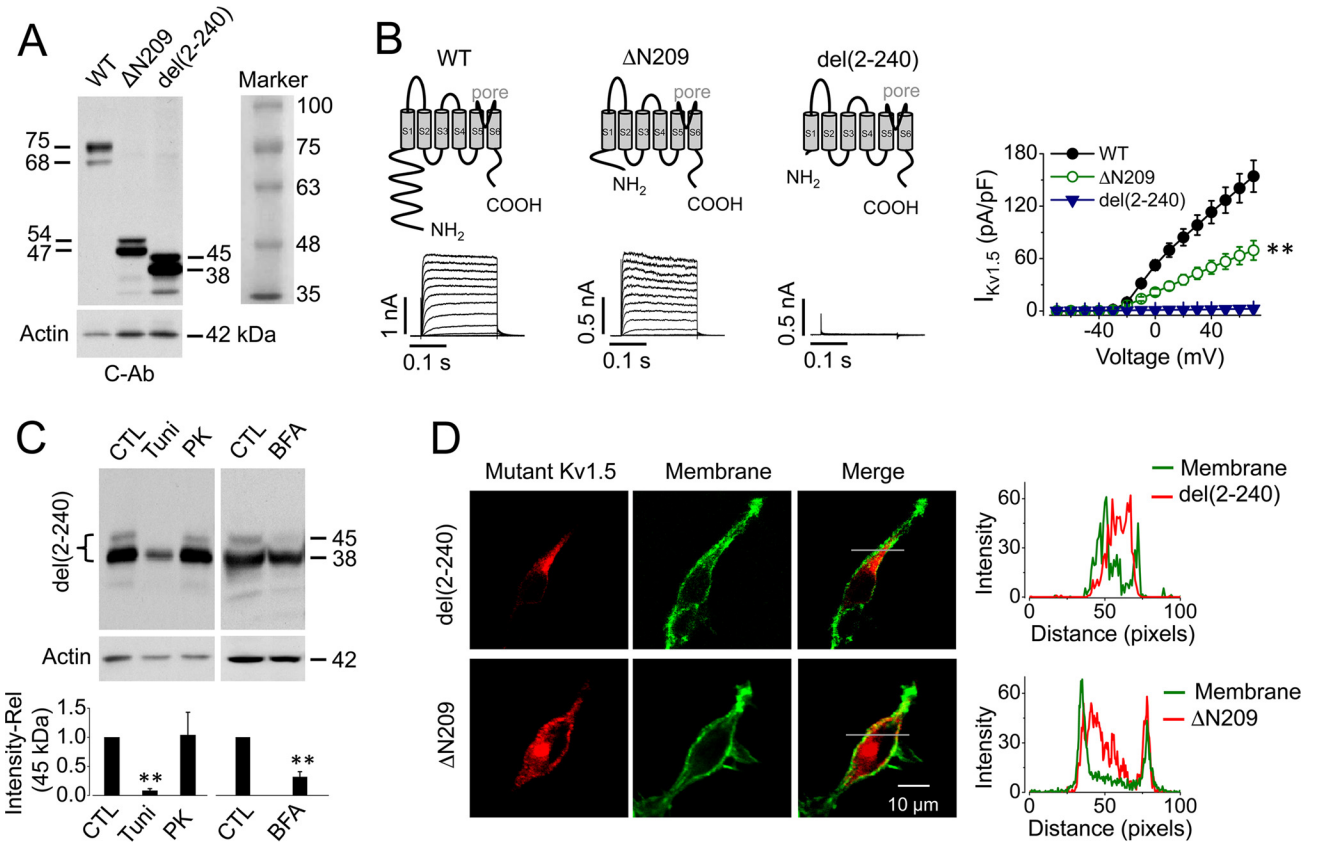

Figure 7. The T1–S1 linker and/or S1 plays a role in Kv1.5 membrane insertion. *A*, Western blots of WT, ΔN209, and del(2–240) Kv1.5 channels expressed in HEK cells ($n = 5$). Molecular mass marker (*Marker*) is shown on the *right*. *B*, schematic illustration of WT, ΔN209, and del(2–240) Kv1.5 channels along with their representative current traces. The voltage protocol was the same as in Fig. 2. On the *right* are summarized *I-V* relationships of WT ($n = 12$), ΔN209 ($n = 6$), and del(2–240) Kv1.5 channels ($n = 8$). **, $p < 0.01$ at −10 mV and above between ΔN209 and WT Kv1.5 currents. *C*, Western blot of del(2–240) Kv1.5 protein from transfected cells cultured in standard condition (*CTL*), with Tuni treatment (10 μg/ml, 48 h), with PK treatment (200 μg/ml, 20 min, 37 °C), or with BFA treatment (10 μM, 12 h). Actin was used as a loading control. Summarized bar graphs are depicted below the representative Western blot images ($n = 4$). *D*, confocal images portraying the cellular location of ΔN209 or del(2–240) Kv1.5 proteins relative to the plasma membrane ($n = 5$). ΔN209 or del(2–240) Kv1.5 proteins were stained with a C-terminal antibody (*C-Ab*) (*red*). Cell membranes are stained *green*. Fluorescence intensities of ΔN209 or del(2–240) Kv1.5 (*red*) and the membrane (*green*) in the *line* across the cell were quantified by ImageJ and are shown on the *right*. *Error bars* represent S.E.

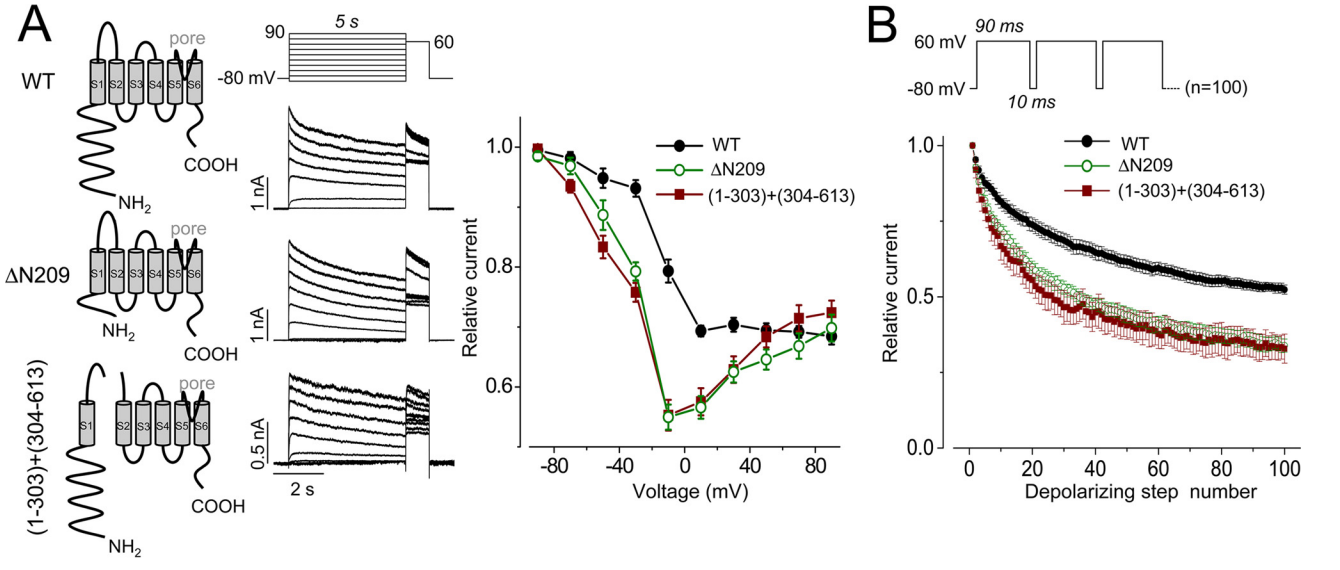

Figure 8. Voltage-dependent inactivation of WT, ΔN209, and Frag(1–303)+(304–613)-coassembled Kv1.5 channels. *A*, *left*, schematic illustration of the channels. *Middle*, representative current traces recorded using the voltage protocol shown above from cells expressing the channels illustrated. The interpulse interval was 15 s. *Right*, voltage dependence of inactivation. Currents at 60 mV were normalized to the maximum value and plotted *versus* the test voltages for WT, ΔN209, and Frag(1–303)+(304–613)-coassembled Kv1.5 channels ($n = 7–11$ cells from three independent experiments for each). *B*, excessive cumulative inactivation of ΔN209 and Frag(1–303)+(304–613)-coassembled Kv1.5 channels compared with WT Kv1.5. The voltage protocol is depicted above plots of normalized current amplitudes against depolarizing steps relative to the value upon the first step ($n = 6–8$ cells for each channel). *Error bars* represent S.E.

length Kv1.5 (Fig. 1*C*). We analyzed the involvement of various regions within Frag(1–303) to further understand Kv1.5 trafficking and function. Our results reveal a novel role of the N terminus in channel assembly: the N terminus can attract and interact with the independent Frag(304–613) to form a functional channel.

A structural element, termed the T1 (tetramerization) domain, within the N terminus of Shaker channels has been suggested to play a central role in the interaction and assembly of channels into homotetrameric or heterotetrameric proteins (28–30). The T1 domain is a module of ~120 amino acids that adopts a "hanging gondola" structure, and its conformation is highly conserved among Kv channel subfamilies (31, 32). However, several reports have demonstrated that Kv channels can still form functional channels upon deletion of the T1 domain (33–35). Nonetheless, the T1 domain has been suggested to impart stability on assembled channels by interactions within the T1 domain or with other channel elements (30). Our data showed that ΔN209 Kv1.5, a naturally occurring isoform of Kv1.5 that lacks most of the T1 domain, is able to generate current (Fig. 7*B*), an observation that is consistent with previous reports (14, 15, 36). However, the present study revealed an important role of amino acid residues 1–209 in channel assembly in the absence of a covalent linkage within the S1–S2 linker. Our data show that Frag(1–209) interacted and associated with Frag(304–613) (Fig. 5*E*). However, this interaction is not sufficient to form a functional channel as Frag(1–209) did not traffic to the membrane (Fig. 5*D*). In contrast, Frag(210–303) facilitated trafficking to the plasma membrane (Fig. 5*D*) but did not interact with Frag(304–613) (Fig. 5*F*). Thus, both Frag(1–209) and (210–303) are required for Frag(304–613) to form a functional channel (Fig. 2). Furthermore, residues 1–209 and 210–303 must be conjoined as a single entity (Frag(1–303)) to assemble with Frag(304–613) and form a functional channel because simultaneous expression of Frag(1–209) and Frag (210–303) with Frag(304–613) did not generate any current (Fig. *5B*). These observations indicate that coexpressed Frag(1–209) and Frag(210–303) could not interact and assemble properly with Frag(304–613) to form a functional channel. This notion is consistent with our data obtained in the dominant-negative suppression experiments (Fig. 6). Frag(1–303) disrupted WT Kv1.5 function. One possible interpretation of this result is that Frag(1–303) is able to assemble with WT subunits to form heterotetrameric channels. Because Frag(1–303) lacks the pore region, its inclusion results in a dominant-negative suppression of WT channels (Fig. 6). In contrast, neither Frag(1–209) nor Frag(210–303) produced a dominant-negative effect on WT Kv1.5 channels (Fig. 6). The lack of dominant-negative suppression of WT Kv1.5 with Frag(210–303) is obvious because it did not interact with Frag(304–613) (Fig. 5*F*). However, although Frag(1–209) interacted with Frag(304–613) (Fig. 5*E*), it did not disrupt WT channels either. We reasoned that, because WT subunits traffic normally, but Frag (1–209) is trafficking-deficient (Fig. 5*D*), they eventually disassociate during maturation and trafficking.

Understanding the dominant-negative effects of Kv1.5 fragments is of biological and clinical importance. Previous reports have demonstrated that overexpression of Kv1.1 polypeptides containing the N terminus and the first transmembrane segment results in a dominant-negative effect on the WT Kv1.5 potassium channel, resulting in arrhythmias (37). A naturally occurring Kv1.5 truncation mutant with a stop codon in amino acid position 375 (conserving the N terminus and S1–S3 segments) was also shown to produce a dominant-negative effect on WT Kv1.5 channels, resulting in atrial fibrillation (17). Our results show that coexpression of Frag(1–303), but not Frag(304–613) (data not shown), with WT Kv1.5 resulted in a dominant-negative suppression of Kv1.5 current (Fig. 6). These observations are consistent with the idea that the T1 domain of the N terminus mediates assembly of Kv channels (28–30). We also observed that the dominant-negative suppression induced by Frag(1–303) was selective to the Kv1.5 channel as the functions of hERG (Kv11.1) and Kv4.3 were unaffected (data not shown). These data support the notion that the presence of the unique N-terminal domain can prevent coassembly between subfamilies (35).

The S1 segment has been shown to play a role in assembly, trafficking, and insertion of Kv channels into the membrane (16, 28, 38, 39). Our results show that Frag(210–303) was able to traffic to the plasma membrane (Fig. 5*D*). Because residues 210–303 contain the S1 segment (residues 248–269), this result may indicate the importance of the S1 segment in channel assembly, trafficking, and membrane expression. Although deletion of the N terminus up to residue 209 (ΔN209) did not disrupt Kv1.5 function, further deletion of amino acid residues 210–240, which removes a region known as the T1–S1 linker of the N terminus, disrupted plasma membrane expression and function (Fig. 7). The T1–S1 linker possesses an α-helical conformation that separates the T1 domain from the S1 transmembrane segment (31, 40). Deletion of this region may have changed the conformation of the S1 segment and thus its hydrophobic nature, preventing membrane expression. Additionally, although both Frag(210–303) and the del(2–240) Kv1.5 channel can traffic through the Golgi apparatus (Figs. 5*C* and 7*C*), only Frag(210–303) was able to insert into the plasma membrane, supporting the notion that the conformation of S1 is disrupted by the del(2–240) mutation. In brief, the finding that Frag(304–613) alone does not reach the plasma membrane (Figs. 2 and 3) but ΔN209 (residues 210–613) does (Fig. 7, *B* and *D*) implies that the T1–S1 linker and/or the S1 segment is important for insertion of Kv1.5 channels into the plasma membrane.

The N terminus and T1 domain also play a role in channel gating. Crystallographic experiments have demonstrated that the T1 domain can assume different conformations, which are responsible for altering voltage-gating characteristics of Kv channels as it aligns with the pore and S4 transmembrane segment (18, 31, 41). In line with this, our results demonstrate that the N-terminal truncation mutant ΔN209 displays a U-shaped voltage dependence of inactivation (Fig. 8), an observation that has been reported previously (14, 15). The whole N terminus is present in Frag(1–303). The fact that Frag(1–303)+(304–613)-coassembled channels display U-shaped voltage dependence of inactivation suggests that that the impact of the N terminus on channel inactivation is lost in Frag(1–303)+(304–613)-coassembled channels (Fig. 8). PK cleavage did not result

in U-shaped voltage dependence of inactivation. Also, although the two PK-produced fragments of WT Kv1.5 did not associate (Fig. 1*C*), the coexpressed Frag(1–303) and Frag(304–613) did associate (Fig. 4), and the N terminus is critical for the association (Fig. 5*E*). Thus, the N terminus of Frag(1–303)+(304–613)-coassembled channels is localized differently than WT channel regardless of PK cleavage, leading to the U-shaped voltage dependence of inactivation (Fig. 8).

In summary, by reconstituting functional Kv1.5 channels using Frag(1–303) and Frag(304–613) (separated at the S1–S2 linker), our study revealed a novel role of the N terminus in channel maturation: the N terminus is powerful enough to attract and interact with the rest of the channel (*i.e.* Frag(304–613)) to form a functional channel independently of the linkage between S1 and S2. Because the S1–S2 linker is usually intact in WT channels, the contribution of the N terminus to channel assembly through targeting the C-terminal side of the channel found in the present study is entirely novel. In addition, our results revealed the importance of the T1–S1 linker and/or S1 segment in plasma membrane expression.

Experimental procedures

Molecular biology

WT Kv1.5 cDNA was provided by Dr. Michael Tamkun (Colorado State University, Fort Collins, CO). For generating plasmids encoding Frag(1–209), Frag(210–303), Frag(1–303), Frag(210–613) (ΔN209), Frag(304–613), and del(2–240), PCR clones of the corresponding inserts from WT Kv1.5 template were constructed in pcDNA3 using BamHI and EcoRI restriction enzymes. The constructs were verified through sequencing across the inserts (GENEWIZ, South Plainfield, NJ). Lipofectamine 2000 was used to transfect WT Kv1.5 and mutant constructs with GFP plasmid into HEK 293 cells. Cell lines stably expressing WT Kv1.5 (Kv1.5-HEK), ΔN209 Kv1.5 (ΔN209 Kv1.5-HEK), or Frag(1–303)+(304–613)-coassembled Kv1.5 were established using G418 for selection (1 mg/ml) and maintenance (0.4 mg/ml). The WT Kv1.5-HEK cell line in the present study displays whole-cell currents in the range of 2000–4000 pA (150–300 pA/pF). These stable cell lines and otherwise indicated transient expressions were used throughout the study. HEK cells were cultured in minimum essential medium (MEM) supplemented with 10% fetal bovine serum, 1 mM sodium pyruvate, and 1× nonessential amino acids (Thermo Fisher Scientific, Waltham, MA). Twenty-four hours after transfection, cells were collected for biochemical and patch clamp experiments. GFP-positive cells were used for whole-cell patch clamp recordings.

Extracellular cleavage of cell-surface proteins

To cleave the extracellularly exposed S1–S2 linker of Kv1.5 channels, the serine protease PK was used. Live Kv1.5-HEK cells or Frag(1–303)+(304–613)-Kv1.5-HEK cells were treated with PK (200 μg/ml in phosphate-buffered saline (PBS) or MEM) for 20 min at 37 °C. Next, PBS containing 6 mM phenylmethylsulfonyl fluoride (PMSF) and 25 mM EDTA was added to terminate the reaction. To determine the effects of PK cleavage on $I_{Kv1.5}$ (Fig. 1*C*), control cells were treated with 0.025% trypsin in PBS for 20 min at 37 °C for collection.

Western blot analysis and coimmunoprecipitation

Western blot analysis was used to detect protein expression of WT, mutants, and fragments of Kv1.5 channels. Cells were washed with ice-cold 1× PBS, collected, and centrifuged at 100 × *g* for 4 min. Next, the cell pellets were lysed using high-frequency sonification in ice-cold lysis buffer containing 1% PMSF and 1% protease inhibitor mixture. The lysates were centrifuged at 10,000 × *g* for 10 min. The protein concentrations were determined using a protein assay kit. Appropriate amounts of double-distilled water and loading buffer containing 5% β-mercaptoethanol were added to the protein to make 0.3 μg/μl samples. Protein samples (15 μg) were loaded and separated on 8, 10, or 15% SDS-polyacrylamide gels and transferred onto polyvinylidene difluoride membranes. BLUeye Prestained Protein Ladder was used to identify the mass of proteins. The membranes were blocked to prevent nonspecific protein interactions with 5% nonfat skim milk and 0.1% Tween 20 in Tris-buffered saline for 1 h at room temperature. Next, membranes were incubated with either 1:1000 N terminus–, 1:500 S1–S2 linker–, or 1:1000 C terminus–specific polyclonal rabbit anti-Kv1.5 primary antibody for 1 h at room temperature. Actin was detected as a loading control using 1:2000 monoclonal mouse anti-actin primary antibody. The membranes were then incubated with goat anti-rabbit (for Kv1.5 detection) or horse anti-mouse (for actin detection) horseradish peroxidase (HRP)-conjugated secondary antibodies for 1 h at room temperature. An enhanced chemiluminescence detection kit was used to visualize the protein bands on X-ray films.

For co-IP, 0.5 mg of whole-cell protein in 0.25 ml of lysis buffer was incubated with appropriate primary antibody overnight at 4 °C. GAPDH was precipitated with rabbit anti-GAPDH primary antibody as a negative control. Protein A/G Plus-agarose beads were then added to the protein complexes for 4 h at 4 °C prior to precipitation by centrifugation at 10,000 × *g* for 1 min. Next, the beads were washed five times with cold lysis buffer before being resuspended in 2× sample buffer. The samples were boiled for 5 min and centrifuged at 20,000 × *g* for 5 min. Finally, the supernatants were loaded into SDS-polyacrylamide gels and subjected to Western blot analysis.

Electrophysiological recordings

A whole-cell patch clamp method was used to record $I_{Kv1.5}$. Cells were settled on the bottom of a 0.5-ml perfusion chamber in the bath solution. Patch glass pipettes were pulled using thin-walled borosilicate glass (World Precision Instruments, Sarasota, FL). The pipettes had inner diameters of 1.5 μm and resistances of 2 megaohms when filled with solution. An Axopatch 200B amplifier and pCLAMP10 (Molecular Devices, San Jose, CA) were used for data acquisition and analysis. Data were sampled at 20 kHz and filtered at 5 kHz. Series resistance was compensated by 80%, and leak subtraction was not used. $I_{Kv1.5}$ was elicited from a holding potential of −80 mV by depolarizing steps to voltages between −70 and +70 mV in 10-mV increments for 200 ms. A repolarizing step to either −50 or −20 mV was applied for 250 ms before returning to the holding potential. To measure the voltage dependence of the channel inacti-

vation, a series of 5-s conditioning pulses to various potentials were followed by a 1-s test pulse to +60 mV. The current amplitudes during the test pulse were plotted against voltages of the conditioning pulses to construct voltage-inactivation relationships. In addition, 100 repetitive depolarization pulses to +60 mV for 90 ms and repolarization to −80 mV for 10 ms were applied continuously to observe excessive cumulative inactivation. The bath solution contained 135 mM NaCl, 5 mM KCl, 1 mM $MgCl_2$, 2 mM $CaCl_2$, 10 mM glucose, and 10 mM HEPES (pH 7.4 with NaOH). The pipette solution consisted of 135 mM KCl, 5 mM MgATP, 5 mM EGTA, and 10 mM HEPES (pH 7.2 with KOH). Patch clamp experiments were performed at room temperature (22 ± 1 °C).

Isolation of cell-surface proteins

To determine the cell-surface localization of the N- and C-fragments, a cell surface protein isolation kit was used to extract membrane proteins from HEK cells expressing the fragments. Cells were grown to 90% confluence in 100-mm culture dishes. Membrane proteins were labeled with a membrane-impermeant thiol-cleavable amine-reactive biotinylation reagent, Sulfo-NHS-SS-biotin, at 250 μg/ml for 30 min at 4 °C. Quenching solution was then added to cease the labeling reaction. Cells with biotinylated surface proteins were collected and lysed with lysis buffer containing 1% protease inhibitor mixture. After centrifugation at 10,000 × *g* for 2 min at 4 °C, biotin-tagged proteins were isolated using NeutrAvidin-agarose columns and eluted with SDS-polyacrylamide sample buffer containing DTT. The isolated cell-surface proteins were analyzed via Western blot analysis. As a loading control, Na^+/K^+-ATPase expression was detected using mouse anti-Na^+/K^+-ATPase α1 antibody and horse anti-mouse HRP-conjugated secondary antibody.

Immunofluorescence microscopy

HEK cells expressing WT Kv1.5, Kv1.5 mutants, or fragments were grown on glass coverslips. Live cell membranes were stained with Oregon Green 488 wheat germ agglutinin (5 μg/ml) for 1 min in Hanks' balanced salt solution. The cells were then fixed using 4% ice-cold paraformaldehyde in PBS for 15 min, permeabilized with 0.1% Triton X-100 for 10 min, and blocked with 5% BSA in PBS for 1 h. WT and mutants of Kv1.5 were labeled with N terminus–, S1–S2 linker–, or C terminus–specific rabbit anti-Kv1.5 primary antibody and Alexa Fluor 594–conjugated donkey anti-rabbit secondary antibody. The coverslips were mounted onto glass slides using Prolong Gold antifade reagent. Images were obtained using a Leica TCS SP2 multiphoton confocal microscope (Leica, Heidelberg, Germany).

Reagents and antibodies

Three different rabbit anti-Kv1.5 polyclonal antibodies targeting specific regions of Kv1.5 were used. An N terminus–specific anti-Kv1.5 antibody (H-120, sc-25681) raised against amino acids 1–120 of Kv1.5 of human origin was purchased from Santa Cruz Biotechnology (Dallas, TX). A C terminus–specific anti-Kv1.5 antibody (APC-004) raised against amino acid residues 513–602 of mouse Kv1.5 (accession number Q61762; 70 of 90 amino acid residues identical to human Kv1.5 amino acids 524–613) was purchased from Alomone Labs (Jerusalem, Israel). An S1–S2 linker–specific anti-Kv1.5 antibody (APC-150) raised against amino acid residues 268–279 of rat Kv1.5 (accession number P19024; 11 of 12 amino acid residues identical to human Kv1.5 amino acids 277–288) was purchased from Alomone Labs. MEM, fetal bovine serum, trypsin, sodium pyruvate, minimal essential amino acids, Lipofectamine 2000, Opti-MEM, Oregon Green 488 wheat germ agglutinin, Hanks' balanced salt solution, and Alexa Fluor 594–conjugated donkey anti-rabbit secondary antibody were purchased from Invitrogen. G418, PMSF, protease inhibitor mixture, brefeldin A, β-mercaptoethanol, proteinase K, Triton X-100, BSA, Prolong Gold antifade mountant, tunicamycin, monoclonal mouse anti-actin (AC-40) antibody (A4700), and all chemicals/electrolytes used in the patch clamp experiments were obtained from Sigma-Aldrich. Rabbit anti-GAPDH (FL-335, sc-25778) and mouse anti-Na^+/K^+-ATPase α1 (sc-21712) primary antibodies and Protein A/G Plus-agarose for immunoprecipitation assays were purchased from Santa Cruz Biotechnology. Horse anti-mouse (7076) and goat anti-rabbit (7074) HRP-conjugated secondary antibodies were purchased from Cell Signaling Technology (Danvers, MA). The BLUeye Prestained Protein Ladder (GeneDirex) was purchased from FroggaBio (Toronto, Ontario, Canada). The cell surface protein isolation kit was purchased from Thermo Fisher Scientific. An enhanced chemiluminescence detection kit was purchased from GE Healthcare. X-ray films were from Fujifilm (Tokyo, Japan). Paraformaldehyde was obtained from Alfa Aesar (Ward Hill, MA).

Author contributions—S. M. L. and S. Z. conceptualization; S. M. L., J. G., and S. Z. data curation; S. M. L., W. L., J. G., T. Y., and S. Z. formal analysis; S. M. L., A. E. H.-C., W. L., J. G., T. Y., J. N. T., and S. Z. investigation; S. M. L. and A. E. H.-C. writing-original draft; S. M. L., A. E. H.-C., W. L., T. Y., J. N. T., and S. Z. writing-review and editing; S. Z. resources; S. Z. supervision; S. Z. funding acquisition; S. Z. project administration.

References

1. Ravens, U., and Wettwer, E. (2011) Ultra-rapid delayed rectifier channels: molecular basis and therapeutic implications. *Cardiovasc. Res.* **89,** 776–785 CrossRef Medline
2. Fedida, D., Wible, B., Wang, Z., Fermini, B., Faust, F., Nattel, S., and Brown, A. M. (1993) Identity of a novel delayed rectifier current from human heart with a cloned K^+ channel current. *Circ. Res.* **73,** 210–216 CrossRef Medline
3. Wang, Z., Fermini, B., and Nattel, S. (1993) Sustained depolarization-induced outward current in human atrial myocytes: evidence for a novel delayed rectifier K^+ current similar to Kv1.5 cloned channel currents. *Circ. Res.* **73,** 1061–1076 CrossRef Medline
4. Wang, J., Juhaszova, M., Rubin, L. J., and Yuan, X. J. (1997) Hypoxia inhibits gene expression of voltage-gated K^+ channel α subunits in pulmonary artery smooth muscle cells. *J. Clin. Investig.* **100,** 2347–2353 CrossRef Medline
5. Archer, S. L., Souil, E., Dinh-Xuan, A. T., Schremmer, B., Mercier, J. C., El Yaagoubi, A., Nguyen-Huu, L., Reeve, H. L., and Hampl, V. (1998) Molecular identification of the role of voltage-gated K^+ channels, Kv1.5 and Kv2.1, in hypoxic pulmonary vasoconstriction and control of resting membrane potential in rat pulmonary artery myocytes. *J. Clin. Investig.* **101,** 2319–2330 CrossRef Medline

6. Jiang, Y., Lee, A., Chen, J., Ruta, V., Cadene, M., Chait, B. T., and MacKinnon, R. (2003) X-ray structure of a voltage-dependent K^+ channel. *Nature* **423,** 33–41 CrossRef Medline
7. MacKinnon, R. (1991) Determination of the subunit stoichiometry of a voltage-activated potassium channel. *Nature* **350,** 232–235 CrossRef Medline
8. Aggarwal, S. K., and MacKinnon, R. (1996) Contribution of the S4 segment to gating charge in the *Shaker* K^+ channel. *Neuron* **16,** 1169–1177 CrossRef Medline
9. Doyle, D. A., Morais Cabral, J., Pfuetzner, R. A., Kuo, A., Gulbis, J. M., Cohen, S. L., Chait, B. T., and MacKinnon, R. (1998) The structure of the potassium channel: molecular basis of K^+ conduction and selectivity. *Science* **280,** 69–77 CrossRef Medline
10. Hogan-Cann, A., Li, W., Guo, J., Yang, T., and Zhang, S. (2016) Proteolytic cleavage in the S1-S2 linker of the Kv1.5 channel does not affect channel function. *Biochim. Biophys. Acta* **1858,** 1082–1090 CrossRef Medline
11. Ficker, E., Dennis, A. T., Wang, L., and Brown, A. M. (2003) Role of the cytosolic chaperones Hsp70 and Hsp90 in maturation of the cardiac potassium channel HERG. *Circ. Res.* **92,** e87–100 CrossRef Medline
12. Guo, J., Massaeli, H., Li, W., Xu, J., Luo, T., Shaw, J., Kirshenbaum, L. A., and Zhang, S. (2007) Identification of I_{Kr} and its trafficking disruption induced by probucol in cultured neonatal rat cardiomyocytes. *J Pharmacol. Exp. Ther.* **321,** 911–920 CrossRef Medline
13. Guo, J., Massaeli, H., Xu, J., Jia, Z., Wigle, J. T., Mesaeli, N., and Zhang, S. (2009) Extracellular K^+ concentration controls cell surface density of I_{Kr} in rabbit hearts and of the HERG channel in human cell lines. *J. Clin. Investig.* **119,** 2745–2757 CrossRef Medline
14. Kurata, H. T., Soon, G. S., and Fedida, D. (2001) Altered state dependence of C-type inactivation in the long and short forms of human Kv1.5. *J. Gen. Physiol.* **118,** 315–332 CrossRef Medline
15. Kurata, H. T., Soon, G. S., Eldstrom, J. R., Lu, G. W., Steele, D. F., and Fedida, D. (2002) Amino-terminal determinants of U-type inactivation of voltage-gated K^+ channels. *J. Biol. Chem.* **277,** 29045–29053 CrossRef Medline
16. Babila, T., Moscucci, A., Wang, H., Weaver, F. E., and Koren, G. (1994) Assembly of mammalian voltage-gated potassium channels: evidence for an important role of the first transmembrane segment. *Neuron* **12,** 615–626 CrossRef Medline
17. Olson, T. M., Alekseev, A. E., Liu, X. K., Park, S., Zingman, L. V., Bienengraeber, M., Sattiraju, S., Ballew, J. D., Jahangir, A., and Terzic, A. (2006) Kv1.5 channelopathy due to KCNA5 loss-of-function mutation causes human atrial fibrillation. *Hum. Mol. Genet.* **15,** 2185–2191 CrossRef Medline
18. Minor, D. L., Lin, Y. F., Mobley, B. C., Avelar, A., Jan, Y. N., Jan, L. Y., and Berger, J. M. (2000) The polar T1 interface is linked to conformational changes that open the voltage-gated potassium channel. *Cell* **102,** 657–670 CrossRef Medline
19. Klemic, K. G., Shieh, C. C., Kirsch, G. E., and Jones, S. W. (1998) Inactivation of Kv2.1 potassium channels. *Biophys. J.* **74,** 1779–1789 CrossRef Medline
20. Bibi, E., and Kaback, H. R. (1990) *In vivo* expression of the *lacY* gene in two segments leads to functional lac permease. *Proc. Natl. Acad. Sci. U.S.A.* **87,** 4325–4329 CrossRef Medline
21. Kobilka, B. K., Kobilka, T. S., Daniel, K., Regan, J. W., Caron, M. G., and Lefkowitz, R. J. (1988) Chimeric α2-, β2-adrenergic receptors: delineation of domains involved in effector coupling and ligand binding specificity. *Science* **240,** 1310–1316 CrossRef Medline
22. Maggio, R., Vogel, Z., and Wess, J. (1993) Reconstitution of functional muscarinic receptors by co-expression of amino- and carboxyl-terminal receptor fragments. *FEBS Lett.* **319,** 195–200 CrossRef Medline
23. Zen, K. H., McKenna, E., Bibi, E., Hardy, D., and Kaback, H. R. (1994) Expression of lactose permease in contiguous fragments as a probe for membrane-spanning domains. *Biochemistry* **33,** 8198–8206 CrossRef Medline
24. Maduke, M., Williams, C., and Miller, C. (1998) Formation of CLC-0 chloride channels from separated transmembrane and cytoplasmic domains. *Biochemistry* **37,** 1315–1321 CrossRef Medline
25. Mo, L., Xiong, W., Qian, T., Sun, H., and Wills, N. K. (2004) Coexpression of complementary fragments of ClC-5 and restoration of chloride channel function in a Dent's disease mutation. *Am. J. Physiol. Cell Physiol.* **286,** C79–C89 CrossRef Medline
26. Schmidt-Rose, T., and Jentsch, T. J. (1997) Reconstitution of functional voltage-gated chloride channels from complementary fragments of CLC-1. *J. Biol. Chem.* **272,** 20515–20521 CrossRef Medline
27. Lamothe, S. M., Guo, J., Li, W., Yang, T., and Zhang, S. (2016) The human ether-a-go-go-related gene (hERG) potassium channel represents an unusual target for protease-mediated damage. *J. Biol. Chem.* **291,** 20387–20401 CrossRef Medline
28. Shen, N. V., Chen, X., Boyer, M. M., and Pfaffinger, P. J. (1993) Deletion analysis of K^+ channel assembly. *Neuron* **11,** 67–76 CrossRef Medline
29. Shen, N. V., and Pfaffinger, P. J. (1995) Molecular recognition and assembly sequences involved in the subfamily-specific assembly of voltage-gated K^+ channel subunit proteins. *Neuron* **14,** 625–633 CrossRef Medline
30. Strang, C., Cushman, S. J., DeRubeis, D., Peterson, D., and Pfaffinger, P. J. (2001) A central role for the T1 domain in voltage-gated potassium channel formation and function. *J. Biol. Chem.* **276,** 28493–28502 CrossRef Medline
31. Gulbis, J. M., Zhou, M., Mann, S., and MacKinnon, R. (2000) Structure of the cytoplasmic β subunit-T1 assembly of voltage-dependent K^+ channels. *Science* **289,** 123–127 CrossRef Medline
32. Kobertz, W. R., Williams, C., and Miller, C. (2000) Hanging gondola structure of the T1 domain in a voltage-gated K^+ channel. *Biochemistry* **39,** 10347–10352 CrossRef Medline
33. Tu, L., Santarelli, V., Sheng, Z., Skach, W., Pain, D., and Deutsch, C. (1996) Voltage-gated K^+ channels contain multiple intersubunit association sites. *J. Biol. Chem.* **271,** 18904–18911 CrossRef Medline
34. Kobertz, W. R., and Miller, C. (1999) K^+ channels lacking the 'tetramerization' domain: implications for pore structure. *Nat. Struct. Biol.* **6,** 1122–1125 CrossRef Medline
35. Lee, T. E., Philipson, L. H., Kuznetsov, A., and Nelson, D. J. (1994) Structural determinant for assembly of mammalian K^+ channels. *Biophys. J.* **66,** 667–673 CrossRef Medline
36. Eldstrom, J., Choi, W. S., Steele, D. F., and Fedida, D. (2003) SAP97 increases Kv1.5 currents through an indirect N-terminal mechanism. *FEBS Lett.* **547,** 205–211 CrossRef Medline
37. London, B., Jeron, A., Zhou, J., Buckett, P., Han, X., Mitchell, G. F., and Koren, G. (1998) Long QT and ventricular arrhythmias in transgenic mice expressing the N terminus and first transmembrane segment of a voltage-gated potassium channel. *Proc. Natl. Acad. Sci. U.S.A.* **95,** 2926–2931 CrossRef Medline
38. Li, M., Jan, Y. N., and Jan, L. Y. (1992) Specification of subunit assembly by the hydrophilic amino-terminal domain of the *Shaker* potassium channel. *Science* **257,** 1225–1230 CrossRef Medline
39. Patel, K. A., Bartoli, K. M., Fandino, R. A., Ngatchou, A. N., Woch, G., Carey, J., and Tanaka, J. C. (2005) Transmembrane S1 mutations in CNGA3 from achromatopsia 2 patients cause loss of function and impaired cellular trafficking of the cone CNG channel. *Invest. Ophthalmol. Vis. Sci.* **46,** 2282–2290 CrossRef Medline
40. Long, S. B., Campbell, E. B., and Mackinnon, R. (2005) Crystal structure of a mammalian voltage-dependent Shaker family K^+ channel. *Science* **309,** 897–903 CrossRef Medline
41. Cushman, S. J., Nanao, M. H., Jahng, A. W., DeRubeis, D., Choe, S., and Pfaffinger, P. J. (2000) Voltage dependent activation of potassium channels is coupled to T1 domain structure. *Nat. Struct. Biol.* **7,** 403–407 CrossRef Medline